Nitric oxide represses photosystem II and NDH-1 in the cyanobacterium *Synechocystis* sp. PCC 6803

Daniel Solymosi [a], Dmitry Shevela [b], Yagut Allahverdiyeva [a*]

[a] Molecular Plant Biology, Department of Life Technologies, University of Turku, Turku FI–20014, Finland

[b] Chemical Biological Centre, Department of Chemistry, Umeå University, 90187 Umeå, Sweden

[*]Corresponding author: allahve@utu.fi

Abstract

Photosynthetic electron transfer comprises a series of light-induced redox reactions catalysed by multiprotein machinery in the thylakoid. These protein complexes possess cofactors susceptible to redox modifications by reactive small molecules. The gaseous radical nitric oxide (NO), a key signalling molecule in green algae and plants, has earlier been shown to bind to Photosystem (PS) II and obstruct electron transfer in plants. The effects of NO on cyanobacterial bioenergetics however, have long remained obscure. In this study, we exposed the model cyanobacterium *Synechocystis* sp. PCC 6803 to NO under anoxic conditions and followed changes in whole-cell fluorescence and oxidoreduction of P700 *in vivo*. Our results demonstrate that NO blocks photosynthetic electron transfer in cells by repressing PSII, PSI, and likely the NDH dehydrogenase-like complex 1 (NDH-1). We propose that iron-sulfur clusters of NDH-1 complex may be affected by NO to such an extent that ferredoxin-derived electron injection to the plastoquinone pool, and thus cyclic electron transfer, may be inhibited. These findings reveal the profound effects of NO on *Synechocystis* cells and demonstrate the importance of controlled NO homeostasis in cyanobacteria.

Keywords

photosynthesis, linear electron transport, nitric oxide, photosystem II, NADH dehydrogenase-like complex 1, cyanobacteria

Introduction

Photosynthetic electron transport (PET) takes place in the thylakoid membrane where the energy of photons is converted to electrochemical potential *via* charge separations in the reaction centres of photosystem (PS) II and PSI. This enables water splitting at the donor side of PSII and the transfer of extracted electron to the primary and secondary electron acceptors Q_A and Q_B, respectively. After double reduction and protonation, Q_BH_2 diffuses to the membrane plastoquinone (PQ) pool. A non-heme iron (NHI) with bound bicarbonate ion (HCO_3^-) is located at the acceptor site of PSII (Ferreira et al., 2004; Umena et al., 2011) interacting with Q_A and Q_B *via* indirect hydrogen-bonding networks. These interactions allow electron (and charge) delocalization between NHI, Q_A, and Q_B, thus regulating Q_A-to-Q_B electron transfer (Müh and Zouni, 2013). Indeed, recent *in vitro* studies demonstrated light-

induced dissociation of the HCO_3^- ligand from its binding site that resulted in a slower Q_A-to-Q_B electron transfer (Brinkert et al., 2016; Shevela et al., 2020). Moreover, based on quantum/molecular mechanical modelling studies, the HCO_3^- ligand seems to assist in the protonation of Q_B (Saito et al., 2013). Electrons from PQH_2 are conveyed *via* cytochrome (Cyt) b_6f, plastocyanin (PC)/ Cyt c_6, and PSI to the cytoplasmic ferredoxin (Fed), a protein which functions as a distribution hub of photosynthetic electrons. In the model cyanobacterium *Synechocystis* sp. PCC 6803 (hereafter *Synechocystis*), photosynthetic and respiratory electron transport chains share the thylakoid (Mullineaux, 2014).

Nitric oxide (NO) is a free radical widely recognized as a key signalling molecule participating in a plethora of physiological processes such as growth and development, abiotic and biotic stress, and nutrient acquisition in plants and green algae (Astier et al., 2021; Kolbert et al., 2019). The primary source of NO in plants and algae is an enzyme called nitrate reductase (Hao et al., 2010; Planchet et al., 2005; Sakihama et al., 2002). Production of NO was also observed in cyanobacteria (Mallick et al., 1999) but the mechanism yet remains to be revealed. A functional L-arginine-dependent NO synthase-like protein was discovered recently in the unicellular cyanobacterium *Synechococcus* sp. 7335 (SyNOS), the encoding gene, however, is rather rare in the genomes of cyanobacteria (Correa-Aragunde et al., 2018). Alternatively, NO may be produced by hemoglobins that convert nitrite to NO under anoxic conditions, as evidenced by *in vitro* studies on hemoglobin isolated from *Synechocystis* (Sturms et al., 2011). Given the lipophilic nature, and high diffusivity in water (~22 $\mu m^2\ s^{-1}$ at 25°C), NO freely penetrates through biological membranes and rapidly disperses within the cells (Hughes, 2008; Zacharia and Deen, 2005). The major mechanism of NO-dependent signalling in oxygenic phototrophs appears to be S-nitrosation, as evidenced by the lack of genes encoding prototypic NO/cGMP signalling proteins in genomes and transcriptomes of green algae and plants, apart from a few species of the *Chlamydomonales* order (Astier et al., 2019). S-nitrosation is a post-translational modification (PTM) predominantly exerted *via* NO-derived molecules, e.g., N_2O_3 formed when NO is oxidized to NO_2 in the presence of O_2 (Eqs. 1,2) (Astier et al., 2011; Hughes, 2008).

$$2\ NO + O_2 \rightarrow 2\ NO_2 \text{ (Equation 1)}$$

$$NO_2 + NO \rightleftharpoons N_2O_3 \text{ (Equation 2)}$$

Molecules of N_2O_3 transfer NO groups to thiolates of Cys residues within proteins forming S-nitrosothiols. Erroneously, S-nitrosation is often represented by the term S-nitrosylation (Gupta et al., 2020). Proteomics studies in *Arabidopsis thaliana* and *Chlamydomonas reinhardtii* (hereafter *Chlamydomonas*) revealed S-nitrosation sites in several proteins participating in photosynthetic electron transfer e.g., subunits of PSI and PSII, Cyt b_6f, Cyt c_6, or enzymes of the CBB cycle such as ribulose bisphosphate carboxylase (Rubisco), fructose 1,6-bisphosphatase and glyceraldehyde 3-phosphate dehydrogenase (GAPDH) (Lindermayr et al., 2005; Morisse et al., 2014). Accordingly, the degradation of Cyt b_6f and Rubisco was shown to be governed by NO in photomixotrophically cultivated

Chlamydomonas cells deprived of N or S, although it remains unclear whether NO acted as a tag or a trigger (De Mia et al., 2019; Wei et al., 2014). Recently, site-specific S-nitrosation was shown to decrease the activity of NAB1, a cytosolic RNA-binding repressor regulating the translation of light-harvesting complex (LHC) protein LhcbM, a subunit of LHCII in *Chlamydomonas* (Berger et al., 2016). These studies demonstrate the potential function of NO in regulating photophysiology *via* S-nitrosation in plants and green algae.

Apart from attacking Cys residues, NO binds to transition metals —such as Fe, Cu, or Mn— forming metal-nitrosyl complexes. Ferrous iron is especially susceptible to NO, the rate constant (k_{on}) of the complex formation between ferrous heme iron and NO ranges between ~ $1*10^6$-10^8 $M^{-1}s^{-1}$ (Ford and Lorkovic, 2002). The photosynthetic apparatus contains several transition metals, especially iron, thus metal-nitrosyl complex formation has profound effects on PET. Earlier *in vitro* studies on isolated spinach thylakoids demonstrated that under anoxic conditions, NO binds to NHI slowing Q_A-to-Q_B electron transfer and decreasing the photochemical efficiency of PSII (Diner and Petrouleas, 1990; Petrouleas and Diner, 1990). Additionally, NO was shown to bind to the Tyr_D residue of the D2 subunit of PSII and the Mn_4CaO_5 cluster in thylakoids isolated from spinach (Goussias et al., 1997; Sanakis et al., 1997). By sequential release and re-binding (Ioannidis et al., 2000), NO is known to reduce the Mn_4CaO_5 cluster and form the so-called "S_{-2} state" of the water-oxidizing complex (WOC), as shown by *in vitro* studies in both spinach thylakoids and PSII complexes of the cyanobacterium *Thermosynechococcus elongatus* (Sarrou et al., 2003; Schansker et al., 2002). These detrimental effects on PSII are reflected in slower light-induced ΔpH formation across the thylakoid membrane *in vitro* (Takahashi and Yamasaki, 2002). Interestingly, exogenous NO in low concentrations reportedly stimulates photosynthesis in plants exposed to different abiotic stresses (Misra et al., 2014; Procházková et al., 2013). Apart from PSII, Cyt b_6f was shown to ligate NO *via* its heme c_i cofactor under anoxic conditions *in vitro* (Twigg et al., 2009). Heme c_i is located at the cytoplasmic side of the complex (Kurisu et al., 2003; Stroebel et al., 2003), and proposedly transfers electrons from Fed to PQ in an alternative Q-cycle (Cramer and Hasan, 2016; Mulkidjanian, 2010) and CET in *Chlamydomonas* (Buchert et al., 2020). The adverse effects of NO on the photochemical reactions were confirmed *in vivo* in plants, the photochemical efficiency of PSII substantially decreased in leaf discs of pea (*Pisum sativum*) and epidermal strips of bean (*Vicia faba*) when exposed to NO donor S-nitrosoglutathione (GNSO) peptides under atmospheric conditions (Ördög et al., 2013; Wodala et al., 2008).

Cyanobacteria possess NO-scavenging enzymes such as the nitric oxide reductase (NorB) that was shown to convert NO to N_2O in *Synechocystis* (Büsch et al., 2002). Active cyanoglobins (GlbN) were isolated from several species e.g., the filamentous *Nostoc commune* UTEX 584, and the unicellular *Synechococcus* sp. PCC 7002 and *Synechocystis* (Scott et al., 2002; Scott and Lecomte, 2008; Thorsteinsson et al., 1999). Cyanoglobins were proven effective against NO stress in *Synechococcus* (Scott et al., 2010) possibly by oxidizing NO to nitrate *via* the NO dioxygenase (NOD) reaction

(Smagghe et al., 2008). To repeat the NOD reaction, cyanoglobins have to be re-reduced. Recently, it was demonstrated *in vitro* that a cognate hemoglobin reductase extracted from *Synechocystis* is able to reduce cyanoglobins, suggesting that an effective NOD system may exist in cyanobacteria (Uppal et al., 2020). These findings demonstrate that cyanobacteria are equipped with defence mechanisms against NO possibly due to exposure to exo- and/or endogenous NO under natural conditions. However, the effects of NO on the photochemical reactions in cyanobacteria—that necessitates such protective mechanisms—is not well understood. In the present study, we sought to uncover how NO affects the photosynthetic machinery in the model cyanobacterium *Synechocystis in vivo*. To avoid the generation of NO_x and focus on the direct effects of NO, we applied anoxic conditions and short (from 10 s to 2 min) NO treatments. We found that NO represses not only PSII, but also PSI, and possibly NDH-1 consequently blocking photosynthetic electron transport.

Results

Effects of NO on photochemical activity of PSII and PSI in *Synechocystis* cells

In order to assess how NO affects the photochemical activity *in vivo*, whole-cell fluorescence and oxidoreduction of P700 were monitored in dark-adapted *Synechocystis* cells under far-red and actinic red light in the absence or the presence of NO (Fig. 1). Changes in the yield of fluorescence are generally ascribed to the dynamics of fluorescence emission by PSII and are principally modulated by the redox state of Q_A (Stirbet et al., 2018). By assessing saturation pulse-induced changes in the fluorescence yield and oxidoreduction of P700, we determined the photochemical efficiencies of PSII and PSI.

Synechocystis cells in the absence of NO demonstrated typical fluorescence traces (Fig. 1A) and P700 oxidoreduction kinetics (Fig. S1). After 10 min of dark pre-incubation, the yield of PSII (Y(II), Fig. 1B) and PSI (Y(I), Fig. 1C) was comparable to what was observed previously under similar conditions (Solymosi et al., 2020). Exposure to dark triggers state I-to state II transition that is accompanied by large fluorescence quenching (Calzadilla et al., 2019; Mullineaux and Allen, 1990). Recently, it was shown that the core of PSII quenches fluorescence emission in state II *via* yet unidentified dissipative processes (Bhatti et al., 2020; Ranjbar Choubeh et al., 2018). To facilitate the transition from state II to state I thus prevent large fluorescence quenching, PSI was preferentially excited by 30-s far-red illumination (indicated by dark red bars in Fig. 1). Indeed, maximal fluorescence upon a saturating pulse in far-red (F_m^{FR}) and also Y(II) were higher than that in the dark (Fig. 1A, B). After the far-red light interval, cells were re-adapted to darkness (shown as black bars in Fig. 1) for 1 min then exposed to actinic red illumination for 3 min at the same photon flux density that was applied for cultivation (shown by red bars). At dark-to-light transition, fluorescence level (F_t) promptly increased then remained relatively steady for the duration of the actinic light (Fig. 1A).

In order to prevent the oxidation of NO to NO_x in the NO-treated cells, the following experiments were performed under anoxic conditions (see Materials and methods). In cells exposed to anoxia and pre-adapted in the dark, minimal fluorescence (F_0) was 16% ± 4% (P = 0.005) higher than in control cells measured under atmospheric air (Fig. S2). Maximal fluorescence in dark-adapted cells (F_m^D) was strongly quenched (Fig. 1A) and PSII yield was 55% ± 3% (P = 8.5 E-7) lower than in the cells measured under atmospheric (i.e., aerobic) conditions (Fig. 1B). In line with this, donor side limitation at PSI was found to be higher under anoxic conditions than under the air, as evidenced by the obtained Y(ND) values (Fig. 1D). Moreover, some limitation at the acceptor side of PSI, Y(NA), was also observed (see Y(NA) data in Fig. S3). These limitations suppressed Y(I) below the level observed under aerobic conditions (Fig. 1C). The results obtained here imply that the PQ-pool is strongly reduced in the dark likely due to substrate (O_2) limitation of respiratory terminal oxidases (RTOs) and flavodiiron proteins (FDPs). These proteins are vital in regulating the redox poise of the photosynthetic apparatus (Nikkanen et al., 2021). In line with this, dark-to-far-red light transition prompted a sharp drop in fluorescence contrary to what was observed in cells measured under aerobic conditions (Fig. 1A). A similar drop has been shown previously in *Synechocystis* mutants deficient in RTOs, Cox, and Cyd (Ermakova et al., 2016). This supports that the PQ-pool is strongly reduced in cells exposed to dark under anoxic conditions. Under anoxic conditions, Y(ND) in the far-red light interval was found to be lower than that under aerobic conditions (Fig. 1D), thus suggesting a more efficient electron supply to PSI under anoxic conditions. Consequently, the Y(I) in far-red illumination was higher under anoxic conditions than that under aerobic conditions (Fig. 1C). This observed effect might have been facilitated by CET. Enhanced CET at dark-to-light transitions was earlier reported in the green algae *Chlamydomonas* exposed to anoxic conditions (Finazzi et al., 1999; Takahashi et al., 2013). It is important to note that the amount of maximal oxidizable P700 (P_m) was comparable to that under aerobic conditions (Fig. S4). When anoxic cells were exposed to actinic light, fluorescence level strongly increased (Fig. 1A) and the effective Y(II) was initially ~ 67% ± 12% lower (P = 1.56 E-5) than that in cells under aerobic conditions (Fig. 1B). Over time, however, fluorescence gradually relaxed and after 2 min of illumination with actinic light, Y(II) was only 36% ± 13% lower (P = 0.005) when compared to that under aerobic conditions (Fig. 1B). This was also reflected by the Y(ND) parameter, which was initially higher than in the cells measured under aerobic conditions but slightly decreased over time (Fig. 1D). Consequently, Y(I) was initially ~18% ± 7% (P = 0.004) lower compared to what was observed under aerobic conditions but later recovered near to the control level (Fig. 1C). The slight improvement in photochemical efficiency in anoxic cells after 4 min illumination might have been elicited by a minor increase in the concentration of O_2 promoting the oxidation of the PQ-pool and P700. Y(II) in the post-illumination dark was somewhat lower compared to that determined by the second pulse in the light (Fig. 1B), possibly due to state I-to-II transition.

In order to elucidate the effects of NO on the redox state of the PQ-pool in the dark, cells were exposed to 20 μM NO under anoxic conditions (NO was added 2 min prior to each measurement during dark adaptation). Importantly, we applied dissolved NO gas that is free of side effects and enables more precise dosing when compared to common chemicals acting as NO donors (Gupta et al., 2020; Mur et al., 2013). We observed that F_0 (Fig. S2) and Y(II) (Fig. 1B) were comparable to those in the untreated anoxic cells, suggesting that NO has no or minor effects on PSII in the dark. Importantly, Y(ND) was ~10% lower in the presence of NO (Fig. 1D) and Y(I) has been restored to the level observed in untreated cells measured under aerobic conditions (Fig. 1C). Thus, presumably, NO limits the reduction of the PQ pool. In line with this, the far-red illumination lowered fluorescence to a lesser extent than in untreated anoxic cells (Fig. 1A), and did not increase F_m when compared to that obtained in darkness (in other words F_m^{FR} was comparable to F_m^{D}). Importantly, NO reinstated Y(ND) in the far-red light (Fig. 1D). These observations may indicate that NO inhibits electron flow into the intersystem chain in the dark and under far-red light. The effects of NO on P_m has been negligible (Fig. S4). When exposed to actinic light, NO-treated cells did not reveal any transient rise of F_t, contrary to that observed in control anoxic cells (Fig. 1A). Most importantly, under actinic light, NO completely suppressed effective Y(II) (Fig. 1B), drastically increasing Y(ND) (Fig. 1D) and, consequently, eliminating effective Y(I) (Fig 1C). The abolished Y(II) observed here is in line with the above-discussed reports demonstrating the harmful effects of NO on PSII (Diner et al., 1991; Schansker et al., 2002, Sarrou et al. 2003). Notably, Y(NA) appeared to be negligible (Fig. S3) although the determination of Y(NA) is ambiguous at such high levels of Y(ND) observed, therefore it is difficult to conclude about the effects of NO on the acceptor side of PSI. Pulses applied in post-illumination dark interval revealed that Y(II) recovered near to the level observed in control anoxic cells. In line with this, Y(ND) has been alleviated when the light faded and, consequently, Y(I) in the post-illumination dark recovered to a level comparable to that in the untreated control cells (Fig. 1C, S1 inlet). This suggests that the effective Y(I) may have been eliminated primarily due to high Y(ND). Thus, NO may affect PSI rather indirectly.

An increase of fluorescence after the termination of actinic light (F_0 rise) reflects the re-reduction of the PQ-pool by NDH-1 in the dark (Mi et al., 1995). Cells exposed to anoxic conditions displayed a higher plateau of post-illumination F_0 than those under atmospheric conditions (Fig. 1E), supporting that the PQ pool is highly reduced in the dark under anoxic conditions. Importantly, the increase in fluorescence was barely noticeable when cells were exposed to NO under anoxic conditions (Fig. 1E), corroborating that NO affects electron transfer from NDH-1 to the PQ-pool.

These *in vivo* observations suggest that NO inhibits the photochemical activity of both PSII and PSI, and thus drastically limits PET in *Synechocystis* cells.

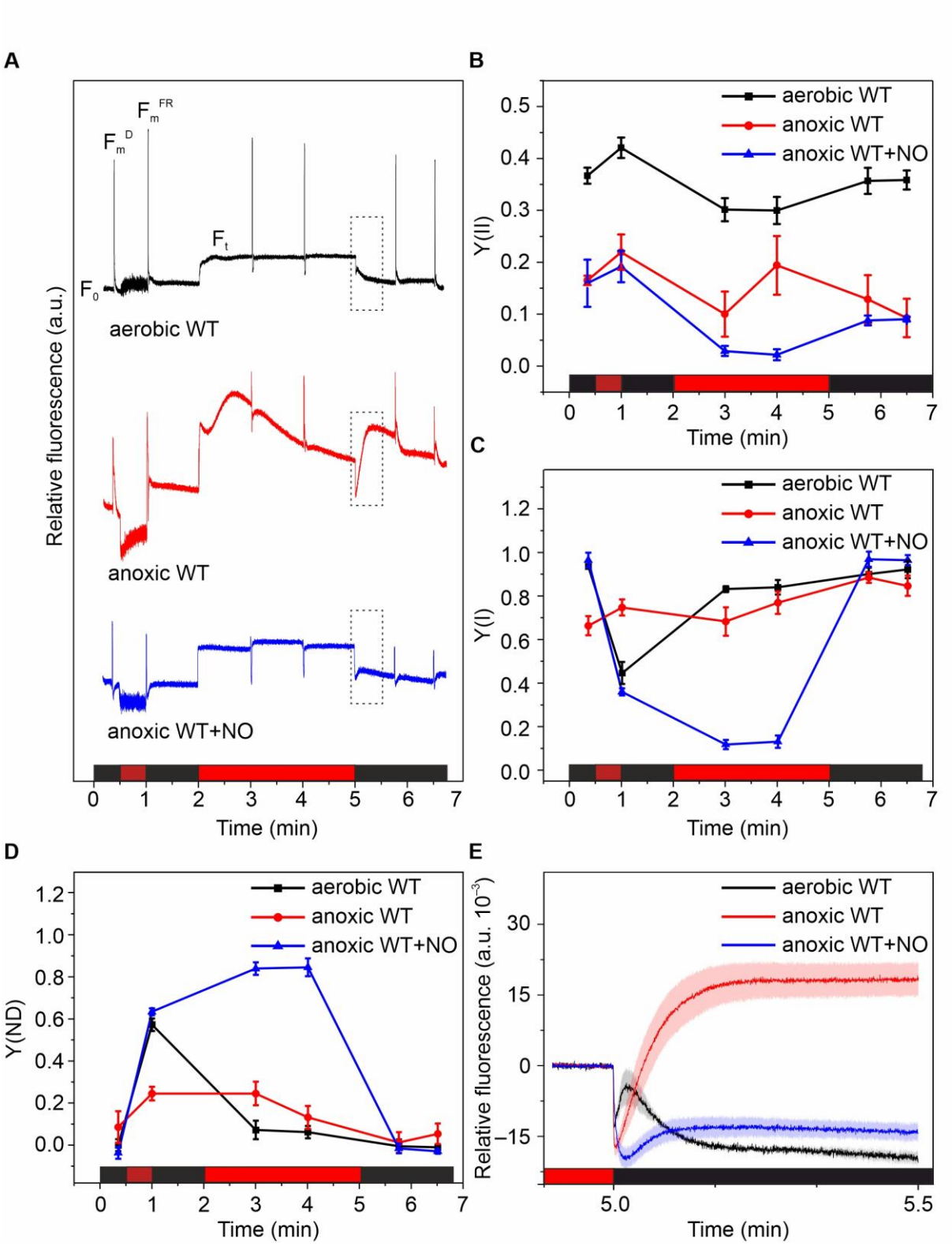

Fig. 1 Characterization of photochemical activity in *Synechocystis* cells. Whole-cell fluorescence (A) was monitored simultaneously with oxidoreduction of P700 to determine Y(II) (B), Y(I) (C) and Y(ND) (D). The cells were exposed to periods of dark (black bars), far-red light (dark-red bars), and 50 μmol photons m^{-2} s^{-1} actinic light (red bars). The measurements were done under aerobic (black traces) and anoxic conditions in the absence (red traces) or in the presence of 20 µM NO (blue traces). Anoxia was established prior to the measurements by supplementing the cells with 10 U ml^{-1} GOx, 20-40 U

ml^{-1} Cat, 5 mM Glc and flushing the headspace with N_2. The cells were incubated in dark for 10 min in total, and NO was added in the eighth min. An increase of fluorescence in the post-illumination dark interval is highlighted with dashed rectangles in panel A and replotted for clarity (E). Traces in panel A are representatives of 4 biological replicates. Y(II), Y(I) and Y(ND) are means ± SD, *n* = 3-4 biological replicates. Traces in panel E are means, the coloured areas indicate SE. a. u., arbitrary units.

Reoxidation of Q_A^- in the presence of NO

The effect of NO on Q_A^- reoxidation in *Synechocystis* cells exposed to anoxic conditions was investigated *in vivo* by following redox kinetics of Q_A in the absence or in the presence of NO. Cells were kept in the dark for 3 min, subjected to a short saturating flash then the decay of the flash-induced fluorescence yield was recorded in the dark. Under anoxic conditions, the cells displayed the waving feature (Fig. 2A; black trace) that was previously described in *Synechocystis* under microoxic conditions and in *Chlamydomonas* under H_2-producing conditions (Deák et al., 2014; Krishna et al., 2019). The wave phenomenon is characterized by an initial decrease of fluorescence yield, corresponding to transient re-oxidation of Q_A^- by Q_B, and a subsequent rise, reflecting the re-reduction of PQ-pool by NDH-1 in the dark (Deák et al., 2014). Strikingly, when cells were exposed to 1 µM or 20 µM NO 10 s prior to the flash, the waving pattern was barely noticeable (Fig. 2A; orange and red traces). The initial decay of fluorescence yield was substantially faster than that in non-treated cells under anoxic conditions (Fig. 2A), indicating accelerated Q_A-to-Q_B electron transfer in the presence of NO, likely due to a more oxidized PQ-pool in the dark. Almost complete elimination of the transient rise (Fig. 2A) indicates that NDH-1 is blocked by NO. It is important to note that the non-treated cells under aerobic conditions displayed a typical monotonous decay (Supplemental Fig. S5) similar to that described previously (Vass et al., 1999). Earlier *in vivo* studies demonstrated that exposing pea leaf disks to NO under atmospheric conditions slows Q_A-to-Q_B electron transfer (Wodala et al., 2008). We observed a similar effect when *Synechocystis* cells were treated with NO under aerobic conditions (Supplemental Fig. S5). In conclusion, the results obtained here clearly indicate that NO blocks electron transfer from NDH-1 to the PQ-pool.

The accelerated Q_A-to-Q_B electron transfer observed here under anoxic conditions (Fig. 2A) likely masks the previously reported detrimental effects of NO on the acceptor side of PSII (Diner and Petrouleas, 1990; Wodala et al., 2008). Therefore, we determined variable fluorescence (F_v, the difference between F_m and F_0) that reflects the formation of Q_A^- upon a flash. We observed that the addition of 1 µM or 20 µM NO decreased F_v under anoxic conditions (Fig. 2B) suggesting that NO hindered the formation of Q_A^- presumably due an altered redox equilibrium of Q_A/Q_A^-.

The effect of NO on the donor side of PSII was evaluated by adding 10 µM 3-(3,4-dichlorophenyl)-1,1-dimethylurea (DCMU) to the cells and monitoring the flash-induced relaxation of fluorescence yield in the absence or in the presence of 20 µM NO under anoxic conditions. DCMU is a well-known herbicide that blocks the Q_A-to-Q_B electron transfer and thus promotes charge recombination between Q_A^- and

the donor-side components. In the absence of NO, DCMU-treated cells under anoxic conditions displayed a typical DCMU-curve (Fig. 2A; blue trace) with dominating component ($t_{1/2}$=2.3 s) arising from recombination between Q_A^- and the WOC in the S_2 state (Vass et al., 1999). When DCMU-treated cells were exposed to NO, clearly two phases ($t_{1/2}$=0.9 s and $t_{1/2}$=53 s) were observed in the relaxation curve (Fig. 2A; green trace). Such long stabilization of the $S_2Q_A^-$ pair could happen due to partial inactivation of the WOC. This indicates that NO perturbs the donor side of PSII. This is in good agreement with previous *in vitro* studies which demonstrated that NO chemically reduces the Mn_4CaO_5 cluster (Sanakis et al., 1997; Sarrou et al. 2003; Schansker et al., 2002). It is important to note that NO decreased F_v value in the presence of DCMU (Fig. 2B), thus likely indicating altered redox state of Q_A in the DCMU-bound PSII complexes.

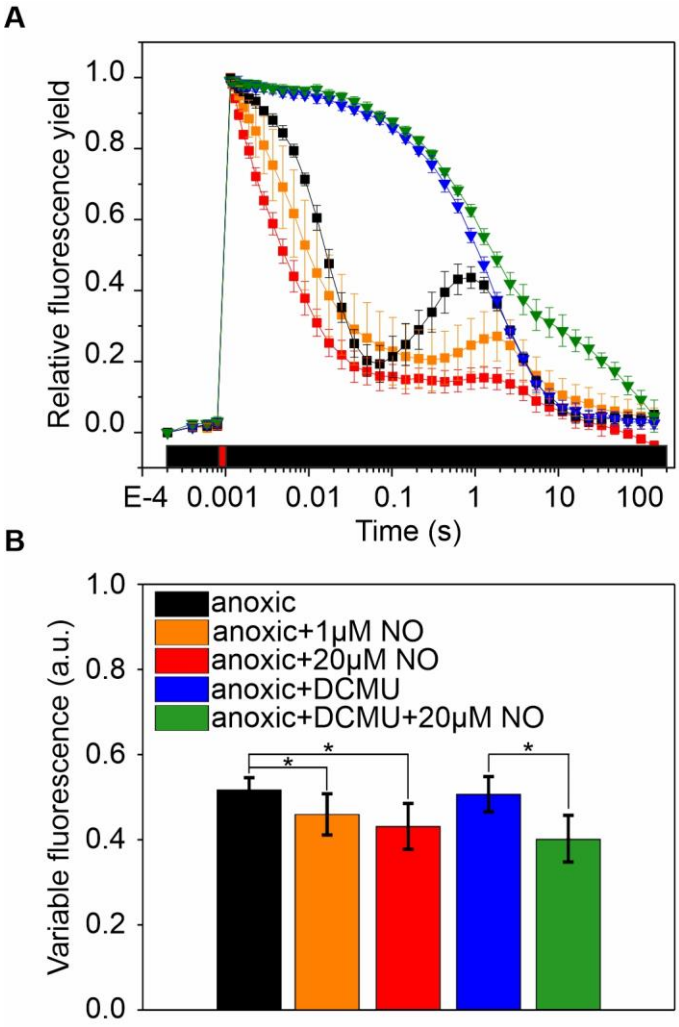

Fig. 2 Relaxation of fluorescence yields after short saturating flash in *Synechocystis* cells. Prior to the measurements, anoxic conditions were established as described in Fig. 1, and then the cells were incubated in the dark for 3 min. The decay of flash-induced fluorescence yield in the dark (A) was monitored in the absence (squares) or the presence of 10 μM DCMU (triangles) without NO (black, blue) or upon exposure of the cells to 1 μM NO (orange) or 20 μM NO (red, green) 10 s prior to the flash. DCMU was added to the cells 30 s prior to flash. Variable fluorescence (F_v) was calculated as the difference between F_m and F_o (B). Means ± SD, n = 3-4 biological replicates, * denotes $P < 0.05$.

Discussion

The effects of NO on photosynthesis in cyanobacterial cells are not well understood. Previous *in vivo* studies focused on higher plants, and by applying various NO donor chemicals (GNSO or sodium nitroprusside), demonstrated that NO decreases the photochemical efficiency of PSII in leaves (Ördög et al., 2013; Wodala et al., 2008; Yang et al., 2004). These studies were performed in the presence of atmospheric O_2 thus it is likely that some NO oxidized into N_2O_3, which partially dissociates in aqueous solutions to produce nitrite (Hughes, 2008). Exogenously added nitrite has been shown to have negligible effects on photosynthesis in leaves (Wodala et al., 2008) but it is known to inhibit PSII in cyanobacterial cells (Zhang et al., 2017). Therefore, we applied anoxic conditions to avoid the production of nitrite and investigate the pure effects of NO on the photosynthetic machinery of cyanobacteria.

By following the emission of whole-cell fluorescence and redox changes of P700 under anoxic conditions, we demonstrated that NO decreases the photochemical efficiency of PSII and PSI and thus limits the flux of photosynthetic electrons in *Synechocystis* cells (Fig. 1, 3A). The functionality of PSI may have been relatively well preserved in the presence of NO, as demonstrated by the recovery of Y(I) to control level in post-illumination darkness (Fig. 1C). This is in line with previous *in vivo* studies showing that the optical cross-section of PSI was unaffected in pea leaves treated with the NO donor GSNO under atmospheric conditions (Wodala and Horváth, 2008).

The molecular mechanisms of PSII inhibition by NO are relatively well understood (Fig. 3B). Earlier *in vitro* studies implicated that NO displaces the bicarbonate ligand of NHI in spinach thylakoids when Q_A is reduced (Diner and Petrouleas, 1990). In the view of more recent data, it is clear that the negative charge of Q_A^- promotes the dissociation of bicarbonate from its binding site at NHI (Brinkert et al., 2016; Shevela et al., 2020), thus providing a free binding site for NO. The release of bicarbonate has been shown to increase E_m of Q_A/Q_A^- (from ~ -145 mV to -70 mV) favouring charge recombination between Q_A^- and P^+ instead of Q_A-to-Q_B electron transfer (Brinkert et al., 2016). Whether NO further modifies the E_m of Q_A/Q_A^- (-70 mV) upon binding to NHI remains to be elucidated through future studies. Nevertheless, the decreased F_v in cells treated with NO (Fig. 2B) as well as the abolished effective Y(II) (Fig. 1B) suggest that the redox state of Q_A is modified. Indeed, the Q_A-to-Q_B electron transfer is known to be slower in plants treated with NO *in vivo* (Wodala et al., 2008). Modification of the acceptor side by NO may lead to a prolonged chlorophyll (chl) triplet state which is linked to the generation of highly toxic singlet oxygen under aerobic conditions (Krieger-Liszkay, 2005; Vass, 2011). In line with this, the production of $^1O_2$ and NO was correlated for *Chlamydomonas* exposed to high light (Chang et al., 2013). Thus, long-term exposure to NO may enhance the rate of PSII photoinhibition. Interestingly, exogenously added bicarbonate was shown to reverse the limitation of PSII by NO both *in vitro* (Diner and Petrouleas, 1990) and *in vivo* (Ördög et al., 2013). This suggests

that depletion of inorganic carbon, that reportedly limits photochemical activity (Holland et al., 2015; Patil et al., 2020), may exacerbate the effects of NO. Therefore, the intracellular bicarbonate level may be an important factor in regulating the impact of NO on PSII complexes in cyanobacteria.

The results obtained in this study show that NO at µM concentration blocks the reduction of the PQ pool driven by NDH-1. This is indicated by the almost complete elimination of the F_0-rise (Fig. 1E) and the wave feature in the relaxation curve of flash-induced fluorescence yield in the presence of NO under anoxic conditions (Fig. 2A). In turn, the oxidized PQ pool may have accelerated electron transfer from Q_A-to-Q_B in the absence of O_2 (Fig. 2A). Previously it has been shown that NO reversibly inhibits mitochondrial NDH in mammals (respiratory complex I), most likely via thiol S-nitrosation (Clementi et al., 1998). However, given that S-nitrosation is an electrophilic attack of NO on thiolates, the oxidation of the radical $NO^{\bullet}$ to the ion NO^+ is a prerequisite (Astier et al., 2011). Since we applied anoxic conditions, oxidation of NO and thus S-nitrosation is unlikely to occur to a considerable extent in our study. We propose that NO blocks NDH-1 by binding to some of the [4Fe-4S] cofactors of the complex (Fig. 3B). Recent reports strongly suggest that [4Fe-4S] clusters mediate electron transfer within NDH-1 from reduced Fed to PQ (Schuller et al., 2019; Zhang et al., 2020). Indeed, it was shown that NDH-1 is the major facilitator of CET in *Synechocystis in vivo* (Miller et al., 2021), NO thus potentially blocks CET in cyanobacteria when exposed to anoxic conditions. The distal [4Fe-4S] cluster (N6a) faces the cytoplasm and can be reached by Fed at a distance of 9.6 Å, and the proximal [4Fe-4S] cluster (N2) is located near the PQ-binding chamber in ~18 Å from the bound PQ (Laughlin et al., 2019; Pan et al., 2020). It is therefore possible that both N6a and N2 are accessible for NO. The binding of NO to FeS-clusters is well documented, with several prokaryotes known to bind NO to FeS proteins (Cruz-Ramos et al., 2002; Ding and Demple, 2000; Singh et al., 2007; Tucker et al., 2010). Nonetheless, the binding of NO to N6a and N2 requires independent verification by structural studies. It is important to note that the physiological concentration of NO in cyanobacteria is yet unknown. Recently, it has been demonstrated that excess exogenous nitrite can promote the release of a few µM of NO in *Chlamydomonas* (Burlacot et al., 2020). It is possible that some accumulation of nitrite triggers the production of NO in cyanobacteria.

In summary, we have demonstrated *in vivo* that NO at µM concentrations limit the flux of photosynthetic electrons in *Synechocystis* cells. We propose that NO, besides affecting WOC and the acceptor side of PSII, stimulates the formation of metal-nitrosyl complexes within NDH-1, thus blocking the electron transfer from Fed to the PQ-pool (Fig 3). The bioenergetic processes of cyanobacteria are thus profoundly affected by NO, necessitating strictly controlled NO homeostasis. The wider metabolism of NO in cyanobacteria remains to be explored.

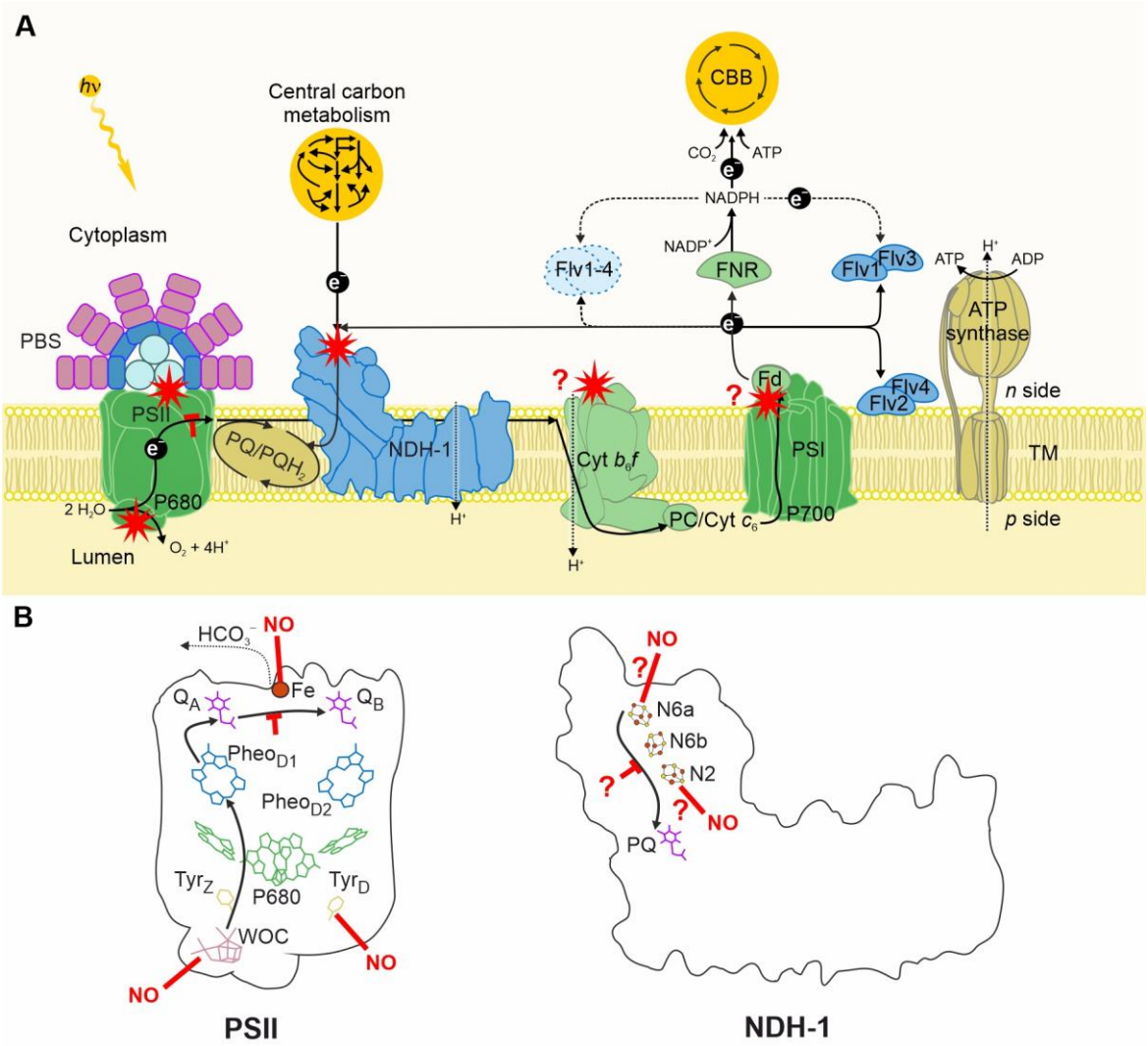

Figure 3 Schematic representation of the proposed target sites of NO in the photosynthetic electron transport chain of *Synechocystis* cells. The flow of water-derived electrons in the thylakoid (A) is repressed by NO via binding to the electron acceptor and electron donor sides of PSII. The PQ pool likely remains oxidized as the electron transfer from Fed to NDH-1 is blocked. Further, NO can modify the heme c_i cofactor residing at the cytoplasmic side of Cyt b_6f or other redox-active sites at the acceptor side of PSI. Thus, combining our results with previously published *in vitro* models of NO-PSII interactions (B), NO represses PSII by binding to the NHI, Tyr_D, and the WOC (namely to the Mn_4CaO_5 cluster). We propose that the target sites of NO at NDH-1 (C) are the [4Fe-4S] clusters ligated by the cytoplasmic arm of the complex. Red stars represent target sites of NO, solid black lines indicate electron fluxes, dashed lines indicate hypothetical electron transfer, short black arrows stand for chemical reactions, dotted lines represent H^+ fluxes, red bars indicate NO-binding sites, red T is to indicate the limitation of the electron transfer, and question marks to show hypothetical effects.

Materials and methods

Cultivation of cyanobacteria

Cells kept in cryogenic storage were revived in liquid BG-11 buffered at pH 7.5 with 20 mM Na-HEPES. Cultures were routinely maintained in 100 mL Erlenmeyer flasks agitated at 120 rpm under constant illumination of 50 µmol photons m^{-2} s^{-1} using an AlgaeTRON AG130 cool-white LED chamber (PSI Instruments) at atmospheric CO_2. For every experiment, pre-cultures were prepared by inoculating pelleted cells at 0.1 OD_{750} in 30 mL BG-11 (pH 7.5) and culturing for 2-3 d under conditions identical to that used for maintaining the cultures. Experimental cultures were then prepared by re-inoculating pelleted pre-culture cells at 0.1 OD_{750} in fresh BG-11 and continuing cultivation for 4 d under the same conditions. Experimental cultures typically reached OD_{750} 0.80±0.072.

Preparation of NO-saturated water for NO treatments

Milli-Q water in a crimp-capped vial (Sigma Aldrich) was flushed first with N_2 (Linde) for 15 min to remove O_2, then with NO gas (purity ≥ 99.5 %, Linde) to saturate the water with NO. The solution was kept on the ice where at 0 °C 0.009833 g NO dissolves in 100 g H_2O (Dean, Lange's Handbook of chemistry), thus a 3.27 mM concentration of NO was calculated. When indicated, dissolved NO gas was added by injecting NO-saturated water into the samples.

Determination of fluorescence and P700 oxidoreduction kinetics

Whole-cell fluorescence and P700 redox kinetics were measured with a pulse-amplitude modulated fluorometer (Dual-PAM-100, Waltz) as it was outlined previously (Solymosi et al., 2020) apart from the following exceptions. Prior to the measurements, chl *a* concentration was adjusted to 15 µg ml^{-1} by resuspending pelleted cells in fresh BG-11 (pH 7.5). Cells were transferred to an airtight quartz cuvette (Hellma) and when necessary, anoxic conditions were established by supplementing the samples with 10 U ml^{-1} GOx (Sigma-Aldrich), 20-40 U ml^{-1} Cat (Sigma-Aldrich), and 5 mM Glc and flushing the headspace with N_2 for 2 min. Dissolved total inorganic carbon concentration was set to 0.5 mM by adding $NaHCO_3$ then 10 min dark incubation was applied. When indicated, NO was added in the 8^{th} min of dark incubation at a final concentration of 20 µM. Drift in the P700 signal was offset by mathematical baseline correction using the Origin 2016 software.

Monitoring changes in flash-induced fluorescence yield in the dark

Relaxation of flash-induced fluorescence yield was determined in an airtight quartz cuvette (Hellma) using a fluorometer (FL3500, PSI Instruments) at room temperature. Samples were adjusted to 5 µg chl ml^{-1} and adapted to dark for 3 min. When indicated, 10 µM DCMU and NO were added 30 s and 10 s prior to the measurements, respectively. A final concentration of 1 µM and 20 µM NO was used. A short (20 µs) saturating flash was applied and the decay of fluorescence yield was followed in dark by weak short (8 µs) measuring flashes for 150 s. Traces were referenced against their respective F_0 and

normalized to F_m. In order to account for the nonlinear correlation between the fluorescence yield and the redox state of Q_A, the obtained fluorescence decay curves were corrected by using the Joliot model (Joliot and Joliot, 1964) with a value of 0.5 for the energy transfer parameter between PSII units. The resulting curves were analysed as described earlier (Allahverdiyeva et al., 2004; Vass et al., 1999) by employing a fitting function with two exponential and one hyperbolic component:

$$F(t) - F_0 = A_1 \exp(-t/T_1) + A_2 \exp(-t/T_2) + A_3/(1 + t/T_3)$$

where F(t) is the variable fluorescence yield, F_0 is the basic fluorescence level before the light flash, A_1–A_3 are the amplitudes, and T_1–T_3 are the time constants. The obtained time constants were used for calculation of the half-lifetimes ($t_{1/2}$) according to $t_{1/2} = T$ (ln 2) for the exponential components and $t_{1/2} = T$ for the hyperbolic component.

Statistical analysis

Statistical significance (P) between means of samples was determined by applying the single factor analysis of variance (ANOVA) method.

Author contributions

Y.A. conceived the project, D.S. and Y.A. designed the research, D.S. performed the experiments, all authors analysed the data, D.S. drafted the manuscript and all authors revised the article.

Acknowledgements

This work was supported by the NordForsk Nordic Center of Excellence "NordAqua" (no. 82845 to Y.A.), the Academy of Finland (project no. 315119 to Y.A), Finnish Academy of Science and Letters (to D.S.) and Doctoral Programme Molecular Life Sciences at the Turku University Graduate school (to D.S.). We thank Tuomas Huokko for assisting in the cultivation of the cells.

Declaration of competing interest

The authors declare that no competing interests influenced the work reported in this paper.

Appendix A Supplementary data

Supplementary Figures S1-5 can be found in Appendix A.

References

Allahverdiyeva, Y., Deák, Z., Szilárd, A., Diner, B.A., Nixon, P.J., Vass, I., 2004. The function of D1-H332 in Photosystem II electron transport studied by thermoluminescence and chlorophyll fluorescence in site-directed mutants of Synechocystis 6803. Eur. J. Biochem. 271, 3523–3532.

Astier, J., Mounier, A., Santolini, J., Jeandroz, S., Wendehenne, D., 2019. The evolution of nitric oxide signalling diverges between animal and green lineages. J. Exp. Bot.

Astier, J., Rasul, S., Koen, E., Manzoor, H., Besson-Bard, A., Lamotte, O., Jeandroz, S., Durner, J., Lindermayr, C., Wendehenne, D., 2011. S-nitrosylation: An emerging post-translational protein

modification in plants. Plant Sci.

Astier, J., Rossi, J., Chatelain, P., Klinguer, A., Besson-Bard, A., Rosnoblet, C., Jeandroz, S., Nicolas-Francès, V., Wendehenne, D., 2021. Nitric oxide production and signalling in algae. J. Exp. Bot. 72, 781–792.

Berger, H., De Mia, M., Morisse, S., Marchand, C.H., Lemaire, S.D., Wobbe, L., Kruse, O., 2016. A light switch based on protein s-nitrosylation fine-tunes photosynthetic light harvesting in chlamydomonas. Plant Physiol. 171, 821–832.

Bhatti, A.F., Choubeh, R.R., Kirilovsky, D., Wientjes, E., van Amerongen, H., 2020. State transitions in cyanobacteria studied with picosecond fluorescence at room temperature. Biochim. Biophys. Acta - Bioenerg. 1861, 148255.

Brinkert, K., De Causmaecker, S., Krieger-Liszkay, A., Fantuzzi, A., Rutherford, A.W., 2016. Bicarbonate-induced redox tuning in Photosystem II for regulation and protection. Proc. Natl. Acad. Sci. U. S. A. 113, 12144–12149.

Buchert, F., Mosebach, L., Gäbelein, P., Hippler, M., 2020. PGR5 is required for efficient Q cycle in the cytochrome b6f complex during cyclic electron flow. Biochem. J. 477, 1631–1650.

Burlacot, A., Richaud, P., Gosset, A., Li-Beisson, Y., Peltier, G., 2020. Algal photosynthesis converts nitric oxide into nitrous oxide. Proc. Natl. Acad. Sci. U. S. A. 117, 2704–2709.

Büsch, A., Friedrich, B., Cramm, R., 2002. Characterization of the norB gene, encoding nitric oxide reductase, in the nondenitrifying cyanobacterium Synechocystis sp. strain PCC6803. Appl. Environ. Microbiol. 68, 668–672.

Calzadilla, P.I., Zhan, J., Sétif, P., Lemaire, C., Solymosi, D., Battchikova, N., Wang, Q., Kirilovskya, D., 2019. The cytochrome b6f complex is not involved in cyanobacterial state transitions. Plant Cell 31, 911–931.

Chang, H.L., Hsu, Y.T., Kang, C.Y., Lee, T.M., 2013. Nitric oxide down-regulation of carotenoid synthesis and psii activity in relation to very high light-induced singlet oxygen production and oxidative stress in chlamydomonas reinhardtii. Plant Cell Physiol. 54, 1296–1315.

Clementi, E., Brown, G.C., Feelisch, M., Moncada, S., 1998. Persistent inhibition of cell respiration by nitric oxide: Crucial role of S-nitrosylation of mitochondrial complex I and protective action of glutathione. Proc. Natl. Acad. Sci. U. S. A. 95, 7631–7636.

Correa-Aragunde, N., Foresi, N., Del Castello, F., Lamattina, L., 2018. A singular nitric oxide synthase with a globin domain found in Synechococcus PCC 7335 mobilizes N from arginine to nitrate. Sci. Rep. 8, 1–11.

Cramer, W.A., Hasan, S.S., 2016. Structure-Function of the Cytochrome b 6 f Lipoprotein Complex. In: Cramer, W. A., Kallas, T. (Eds.), Cytochrome Complexes: Evolution, Structures, Energy Transduction, and Signaling. Springer Netherlands, pp. 177–207.

Cruz-Ramos, H., Crack, J., Wu, G., Hughes, M.N., Scott, C., Thomson, A.J., Green, J., Poole, R.K., 2002. NO sensing by FNR: Regulation of the Escherichia coli NO-detoxifying flavohaemoglobin, Hmp. EMBO J. 21, 3235–3244.

De Mia, M., Lemaire, S.D., Choquet, Y., Wollmana, F.A., 2019. Nitric oxide remodels the photosynthetic apparatus upon S- starvation in Chlamydomonas reinhardtii. Plant Physiol. 179, 718–731.

Deák, Z., Sass, L., Kiss, É., Vass, I., 2014. Characterization of wave phenomena in the relaxation of flash-induced chlorophyll fluorescence yield in cyanobacteria. Biochim. Biophys. Acta -

Bioenerg. 1837, 1522–1532.

Diner, B.A., Petrouleas, V., 1990. Formation by NO of nitrosyl adducts of redox components of the Photosystem II reaction center. II. Evidence that HCO-3/CO2 binds to the acceptor-side non-heme iron. BBA - Bioenerg. 1015, 141–149.

Diner, B.A., Petrouleas, V., Wendoloski, J.J., 1991. The iron-quinone electron-acceptor complex of photosystem II. Physiol. Plant. 81, 423–436.

Ding, H., Demple, B., 2000. Direct nitric oxide signal transduction via nitrosylation of iron-sulfur centers in the SoxR transcription activator. Proc. Natl. Acad. Sci. U. S. A. 97, 5146–5150.

Ermakova, M., Huokko, T., Richaud, P., Bersanini, L., Howe, C.J., Lea-Smith, D.J., Peltier, G., Allahverdiyeva, Y., 2016. Distinguishing the roles of thylakoid respiratory terminal oxidases in the cyanobacterium Synechocystis sp. PCC 6803. Plant Physiol. 171, 1307–1319.

Ferreira, K.N., Iverson, T.M., Maghlaoui, K., Barber, J., Iwata, S., 2004. Architecture of the Photosynthetic Oxygen-Evolving Center. Science (80-.). 303, 1831–1838.

Finazzi, G., Furia, A., Barbagallo, R.P., Forti, G., 1999. State transitions, cyclic and linear electron transport and photophosphorylation in Chlamydomonas reinhardtii. Biochim. Biophys. Acta - Bioenerg. 1413, 117–129.

Ford, P.C., Lorkovic, I.M., 2002. Mechanistic aspects of the reactions of nitric oxide with transition-metal complexes. Chem. Rev. 102, 993–1017.

Goussias, C., Ioannidis, N., Petrouleas, V., 1997. Low-temperature nteractions of NO with the S1 and S2 states of the water-oxidizing complex of photosystem II. A novel Mn-multiline EPR signal derived from the S1 state. Biochemistry 36, 9261–9266.

Gupta, K.J., Hancock, J.T., Petrivalsky, M., Kolbert, Z., Lindermayr, C., Durner, J., Barroso, J.B., Palma, J.M., Brouquisse, R., Wendehenne, D., Corpas, F.J., Loake, G.J., 2020. Recommendations on terminology and experimental best practice associated with plant nitric oxide research. New Phytol. 225, 1828–1834.

Hao, F., Zhao, S., Dong, H., Zhang, H., Sun, L., Miao, C., 2010. Nia1 and nia2 are involved in exogenous salicylic acid-induced nitric oxide generation and stomatal closure in arabidopsis. J. Integr. Plant Biol. 52, 298–307.

Holland, S.C., Kappell, A.D., Burnap, R.L., 2015. Redox changes accompanying inorganic carbon limitation in Synechocystis sp. PCC 6803. Biochim. Biophys. Acta - Bioenerg. 1847, 355–363.

Hughes, M.N., 2008. Chemistry of Nitric Oxide and Related Species. In: Methods in Enzymology. Academic Press Inc., pp. 3–19.

Ioannidis, N., Schansker, G., Barynin, V. V., Petrouleas, V., 2000. Interaction of nitric oxide with the oxygen evolving complex of photosystem II and manganese catalase: A comparative study. J. Biol. Inorg. Chem. 5, 354–363.

Joliot, A., Joliot, P., 1964. Etude cinetique de la reaction photochimique liberant l'oxygene au cours de la photosynthese. Hebd Seances Acad Sci 258, 4622–4625.

Kolbert, Z., Barroso, J.B., Brouquisse, R., Corpas, F.J., Gupta, K.J., Lindermayr, C., Loake, G.J., Palma, J.M., Petřivalský, M., Wendehenne, D., Hancock, J.T., 2019. A forty year journey: The generation and roles of NO in plants. Nitric Oxide - Biol. Chem.

Krieger-Liszkay, A., 2005. Singlet oxygen production in photosynthesis. In: Journal of Experimental Botany. Oxford Academic, pp. 337–346.

Krishna, P.S., Styring, S., Mamedov, F., 2019. Photosystem ratio imbalance promotes direct sustainable H2 production in: Chlamydomonas reinhardtii. Green Chem. 21, 4683–4690.

Kurisu, G., Zhang, H., Smith, J.L., Cramer, W.A., 2003. Structure of the Cytochrome b6f Complex of Oxygenic Photosynthesis: Tuning the Cavity. Science (80-.). 302, 1009–1014.

Laughlin, T.G., Bayne, A.N., Trempe, J.F., Savage, D.F., Davies, K.M., 2019. Structure of the complex I-like molecule NDH of oxygenic photosynthesis. Nature 566, 411–414.

Lindermayr, C., Saalbach, G., Durner, J., 2005. Proteomic identification of S-nitrosylated proteins in arabidopsis. Plant Physiol. 137, 921–930.

Mallick, N., Rai, L.C., Mohn, F.H., Soeder, C.J., 1999. Studies on nitric oxide (NO) formation by the green alga Scenedesmus obliquus and the diazotrophic cyanobacterium Anabaena doliolum. Chemosphere 39, 1601–1610.

Mi, H., Endo, T., Ogawa, T., Asada, K., 1995. Thylakoid membrane-bound, nadph-specific pyridine nucleotide dehydrogenase complex mediates cyclic electron transport in the cyanobacterium synechocystis sp. PCC 6803. Plant Cell Physiol. 36, 661–668.

Miller, N.T., Vaughn, M.D., Burnap, R.L., 2021. Electron flow through NDH-1 complexes is the major driver of cyclic electron flow-dependent proton pumping in cyanobacteria. Biochim. Biophys. Acta - Bioenerg. 1862, 148354.

Misra, A.N., Vladkova, R., Singh, R., Misra, M., Dobrikova, A.G., Apostolova, E.L., 2014. Action and target sites of nitric oxide in chloroplasts. Nitric Oxide - Biol. Chem.

Morisse, S., Zaffagnini, M., Gao, X.H., Lemaire, S.D., Marchand, C.H., 2014. Insight into protein S-nitrosylation in Chlamydomonas reinhardtii. Antioxid. Redox Signal. 21, 1271–1284.

Müh, F., Zouni, A., 2013. The nonheme iron in photosystem II. Photosynth. Res.

Mulkidjanian, A.Y., 2010. Activated Q-cycle as a common mechanism for cytochrome bc1 and cytochrome b6f complexes. Biochim. Biophys. Acta - Bioenerg.

Mullineaux, C.W., 2014. Co-existence of photosynthetic and respiratory activities in cyanobacterial thylakoid membranes. Biochim. Biophys. Acta - Bioenerg. 1837, 503–511.

Mullineaux, C.W., Allen, J.F., 1990. State 1-State 2 transitions in the cyanobacterium Synechococcus 6301 are controlled by the redox state of electron carriers between Photosystems I and II. Photosynth. Res. 23, 297–311.

Mur, L.A.J., Mandon, J., Persijn, S., Cristescu, S.M., Moshkov, I.E., Novikova, G. V., Hall, M.A., Harren, F.J.M., Hebelstrup, K.H., Gupta, K.J., 2013. Nitric oxide in plants: An assessment of the current state of knowledge. AoB Plants.

Nikkanen, L., Solymosi, D., Jokel, M., Allahverdiyeva, Y., 2021. Regulatory electron transport pathways of photosynthesis in cyanobacteria and microalgae: Recent advances and biotechnological prospects. Physiol. Plant. 173, 514–525.

Ördög, A., Wodala, B., Rózsavölgyi, T., Tari, I., Horváth, F., 2013. Regulation of guard cell photosynthetic electron transport by nitric oxide. J. Exp. Bot. 64, 1357–1366.

Pan, X., Cao, D., Xie, F., Xu, F., Su, X., Mi, H., Zhang, X., Li, M., 2020. Structural basis for electron transport mechanism of complex I-like photosynthetic NAD(P)H dehydrogenase. Nat. Commun. 11, 1–11.

Patil, P.P., Vass, I., Kodru, S., Szabó, M., 2020. A multi-parametric screening platform for

photosynthetic trait characterization of microalgae and cyanobacteria under inorganic carbon limitation. PLoS One 15, e0236188.

Petrouleas, V., Diner, B.A., 1990. Formation by NO of nitrosyl adducts of redox components of the Photosystem II reaction center. I. NO binds to the acceptor-side non-heme iron. BBA - Bioenerg. 1015, 131–140.

Planchet, E., Gupta, K.J., Sonoda, M., Kaiser, W.M., 2005. Nitric oxide emission from tobacco leaves and cell suspensions: Rate limiting factors and evidence for the involvement of mitochondrial electron transport. Plant J. 41, 732–743.

Procházková, D., Haisel, D., Wilhelmová, N., Pavlíková, D., Száková, J., 2013. Effects of exogenous nitric oxide on photosynthesis. Photosynthetica.

Ranjbar Choubeh, R., Wientjes, E., Struik, P.C., Kirilovsky, D., van Amerongen, H., 2018. State transitions in the cyanobacterium Synechococcus elongatus 7942 involve reversible quenching of the photosystem II core. Biochim. Biophys. Acta - Bioenerg. 1859, 1059–1066.

Saito, K., Rutherford, A.W., Ishikita, H., 2013. Mechanism of proton-coupled quinone reduction in Photosystem II. Proc. Natl. Acad. Sci. U. S. A.

Sakihama, Y., Nakamura, S., Yamasaki, H., 2002. Nitric oxide production mediated by nitrate reductase in the green alga Chlamydomonas reinhardtii: An alternative NO production pathway in photosynthetic organisms. Plant Cell Physiol. 43, 290–297.

Sanakis, Y., Goussias, C., Mason, R.P., Petrouleas, V., 1997. No interacts with the tyrosine radical Y(D)· of photosystem II to form an iminoxyl radical. Biochemistry 36, 1411–1417.

Sarrou, J., Isgandarova, S., Kern, J., Zouni, A., Renger, G., Lubitz, W., Messinger, J., 2003. Nitric oxide-induced formation of the S-2 state in the oxygen-evolving complex of photosystem II from Synechococcus elongatus. Biochemistry 42, 1016–1023.

Schansker, G., Goussias, C., Petrouleas, V., William Rutherford, A., 2002. Reduction of the Mn cluster of the water-oxidizing enzyme by nitric oxide: Formation of an S-2 state. Biochemistry 41, 3057–3064.

Schuller, J.M., Birrell, J.A., Tanaka, H., Konuma, T., Wulfhorst, H., Cox, N., Schuller, S.K., Thiemann, J., Lubitz, W., Sétif, P., Ikegami, T., Engel, B.D., Kurisu, G., Nowaczyk, M.M., 2019. Structural adaptations of photosynthetic complex I enable ferredoxin-dependent electron transfer. Science (80-.). 363, 257–260.

Scott, N.L., Falzone, C.J., Vuletich, D.A., Zhao, J., Bryant, D.A., Lecomte, J.T.J., 2002. Truncated hemoglobin from the cyanobacterium Synechococcus sp. PCC 7002: Evidence for hexacoordination and covalent adduct formation in the ferric recombinant protein. Biochemistry 41, 6902–6910.

Scott, N.L., Lecomte, J.T.J., 2008. Cloning, expression, purification, and preliminary characterization of a putative hemoglobin from the cyanobacterium synechocystis sp. PCC 6803. Protein Sci. 9, 587–597.

Scott, N.L., Xu, Y., Shen, G., Vuletich, D.A., Falzone, C.J., Li, Z., Ludwig, M., Pond, M.P., Preimesberger, M.R., Bryant, D.A., Lecomte, J.T.J., 2010. Functional and structural characterization of the 2/2 Hemoglobin from Synechococcus sp. PCC 7002. Biochemistry 49, 7000–7011.

Shevela, D., Do, H.N., Fantuzzi, A., Rutherford, A.W., Messinger, J., 2020. Bicarbonate-Mediated CO2Formation on Both Sides of Photosystem II. Biochemistry 59, 2442–2449.

Singh, A., Guidry, L., Narasimhulu, K. V., Mai, D., Trombley, J., Redding, K.E., Giles, G.I., Lancaster, J.R., Steyn, A.J.C., 2007. Mycobacterium tuberculosis WhiB3 responds to O2 and nitric oxide via its [4Fe-4S] cluster and is essential for nutrient starvation survival. Proc. Natl. Acad. Sci. U. S. A. 104, 11562–11567.

Smagghe, B.J., Trent, J.T., Hargrove, M.S., 2008. NO dioxygenase activity in hemoglobins is ubiquitous in vitro, but limited by reduction in vivo. PLoS One 3, e2039.

Solymosi, D., Nikkanen, L., Muth-Pawlak, D., Fitzpatrick, D., Vasudevan, R., Howe, C.J., Lea-Smith, D.J., Allahverdiyeva, Y., 2020. Cytochrome CMdecreases photosynthesis under photomixotrophy in synechocystis sp. PCC 6803. Plant Physiol. 183, 700–716.

Stirbet, A., Lazár, D., Papageorgiou, G.C., Govindjee, 2018. Chlorophyll a Fluorescence in Cyanobacteria: Relation to Photosynthesis. Cyanobacteria From Basic Sci. to Appl. 79–130.

Stroebel, D., Choquet, Y., Popot, J.L., Picot, D., 2003. An atypical haem in the cytochrome b6f complex. Nature 426, 413–418.

Sturms, R., Dispirito, A.A., Hargrove, M.S., 2011. Plant and cyanobacterial hemoglobins reduce nitrite to nitric oxide under anoxic conditions. Biochemistry 50, 3873–3878.

Takahashi, H., Clowez, S., Wollman, F.A., Vallon, O., Rappaport, F., 2013. Cyclic electron flow is redox-controlled but independent of state transition. Nat. Commun. 4, 1–8.

Takahashi, S., Yamasaki, H., 2002. Reversible inhibition of photophosphorylation in chloroplasts by nitric oxide. FEBS Lett. 512, 145–148.

Thorsteinsson, M. V, Bevan, D.R., Potts, M., Dou, Y., Eich, R.F., Hargrove, M.S., Gibson, Q.H., Olson, J.S., 1999. A cyanobacterial hemoglobin with unusual ligand binding kinetics and stability properties. Biochemistry 38, 2117–2126.

Tucker, N.P., Le Brun, N.E., Dixon, R., Hutchings, M.I., 2010. There's NO stopping NsrR, a global regulator of the bacterial NO stress response. Trends Microbiol.

Twigg, A.I., Baniulis, D., Cramer, W.A., Hendrich, M.P., 2009. EPR detection of an O2 surrogate bound to heme cn of the cytochrome b6f complex. J. Am. Chem. Soc. 131, 12536–12537.

Umena, Y., Kawakami, K., Shen, J.R., Kamiya, N., 2011. Crystal structure of oxygen-evolving photosystem II at a resolution of 1.9Å. Nature 473, 55–60.

Uppal, S., Khan, M.A., Kundu, S., 2020. Identification and characterization of a recombinant cognate hemoglobin reductase from Synechocystis sp. PCC 6803. Int. J. Biol. Macromol. 162, 1054–1063.

Vass, I., 2011. Role of charge recombination processes in photodamage and photoprotection of the photosystem II complex. Physiol. Plant. 142, 6–16.

Vass, I., Kirilovsky, D., Etienne, A.L., 1999. UV-B radiation-induced donor- and acceptor-side modifications of photosystem II in the cyanobacterium Synechocystis sp. PCC 6803. Biochemistry 38, 12786–12794.

Wei, L., Derrien, B., Gautier, A., Houille-Vernes, L., Boulouis, A., Saint-Marcoux, D., Malnoë, A., Rappaport, F., de Vitry, C., Vallon, O., Choquet, Y., Wollman, F.A., 2014. Nitric oxide-triggered remodeling of chloroplast bioenergetics and thylakoid proteins upon nitrogen starvation in Chlamydomonas reinhardtii. Plant Cell 26, 353–372.

Wodala, B., Deák, Z., Vass, I., Erdei, L., Altorjay, I., Horváth, F., 2008. In vivo target sites of nitric oxide in photosynthetic electron transport as studied by chlorophyll fluorescence in pea leaves.

Plant Physiol. 146, 1920–1927.

Wodala, B., Horváth, F., 2008. The effect of exogenous NO on PSI photochemistry in intact pea leaves. Acta Biol. Szeged. 52, 243–245.

Yang, J.D., Zhao, H.L., Zhang, T.H., Yun, J.F., 2004. Effects of exogenous nitric oxide on photochemical activity of photosystem II in potato leaf tissue under non-stress condition. Acta Bot. Sin. 46, 1009–1014.

Zacharia, I.G., Deen, W.M., 2005. Diffusivity and solubility of nitric oxide in water and saline. Ann. Biomed. Eng. 33, 214–222.

Zhang, C., Shuai, J., Ran, Z., Zhao, J., Wu, Z., Liao, R., Wu, J., Ma, W., Lei, M., 2020. Structural insights into NDH-1 mediated cyclic electron transfer. Nat. Commun. 11, 1–13.

Zhang, X., Ma, F., Zhu, X., Zhu, J., Rong, J., Zhan, J., Chen, H., He, C., Wang, Q., 2017. The acceptor side of photosystem II is the initial target of nitrite stress in Synechocystis sp. strain PCC 6803. Appl. Environ. Microbiol. 83.

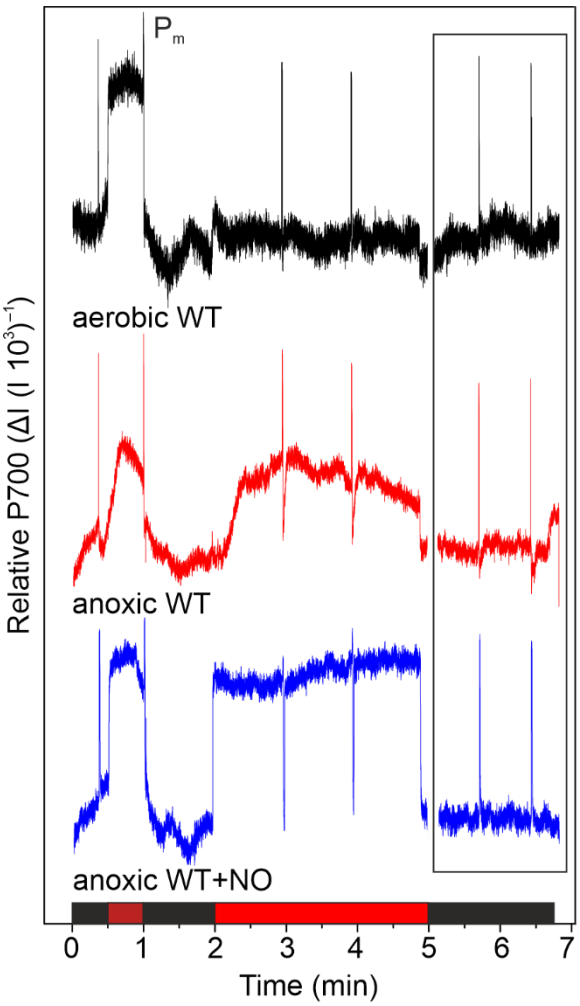

Fig S1. Redox changes of P700 in *Synechocystis* cells. Kinetics of P700 oxidoreduction were followed simultaneously with fluorescence shown in Fig. 1A. For clarity, the post-illumination kinetics are visualized in inlet. Traces are representatives of 3 biological replicates. P_m indicates the pulse at which amount of maximal oxidizable P700 was determined.

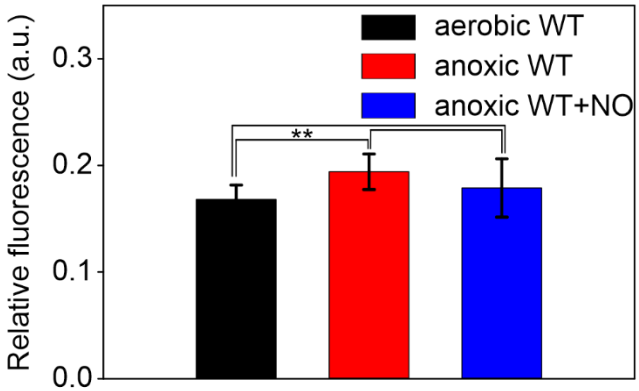

Fig. S2. Minimal fluorescence in *Synechocystis* cells. Minimal fluorescence (F_0) was determined as described prior to the periods of far red and actinic light shown in Fig. 1. Due to the slight variation of

signal intensity between biological replicates, statistical significance was determined by Students' T test (** < 0.005). Values are ± SD, n = 4 biological replicates.

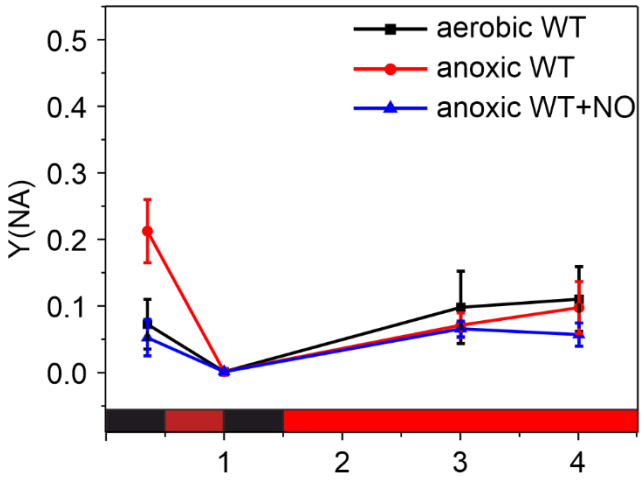

Fig. S3. Acceptor side limitation of PSI. Y(NA) was determined with Y(I) and Y(ND) shown in Fig 1C and D, respectively.

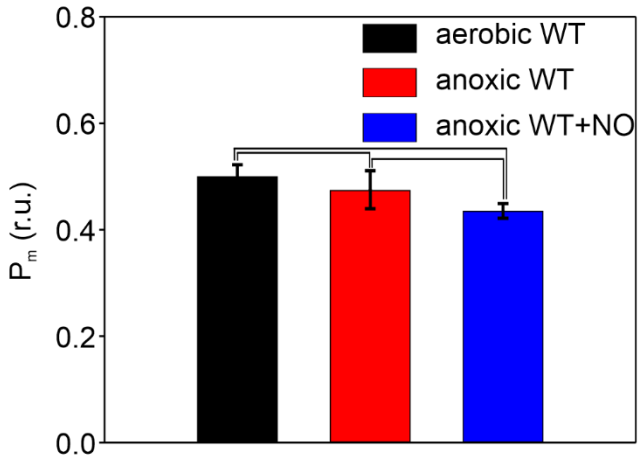

Fig. S4. Maximal oxidizable P700 (P_m). P700 was fully oxidized under strong far red illumination by a saturating multiple turnover flash denotated with P_m in Supplementary Fig. S1. R.u., relative unit.

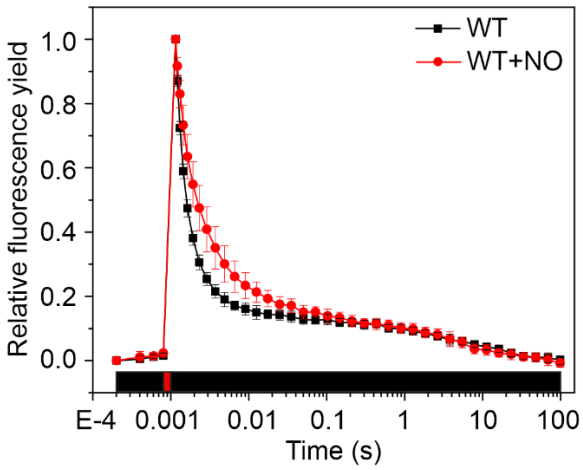

Supplemental Fig. S5. Decay of flash-induced fluorescence yield in the dark under atmospheric conditions. Sample preparation, treatment of the cells and the measurement was carried out as described in Fig. 2 except that here, Gox, Cat and glc and purging with N_2 was not applied.